Supplemental Data

NF-κB/TNF-α positive feedback loop supports myeloid leukemia initiating cell capacity

Yuki Kagoya, Akihide Yoshimi, Keisuke Kataoka, Masahiro Nakagawa, Keiki Kumano, Shunya Arai, Hiroshi Kobayashi, Taku Saito, Yoichiro Iwakura, Mineo Kurokawa

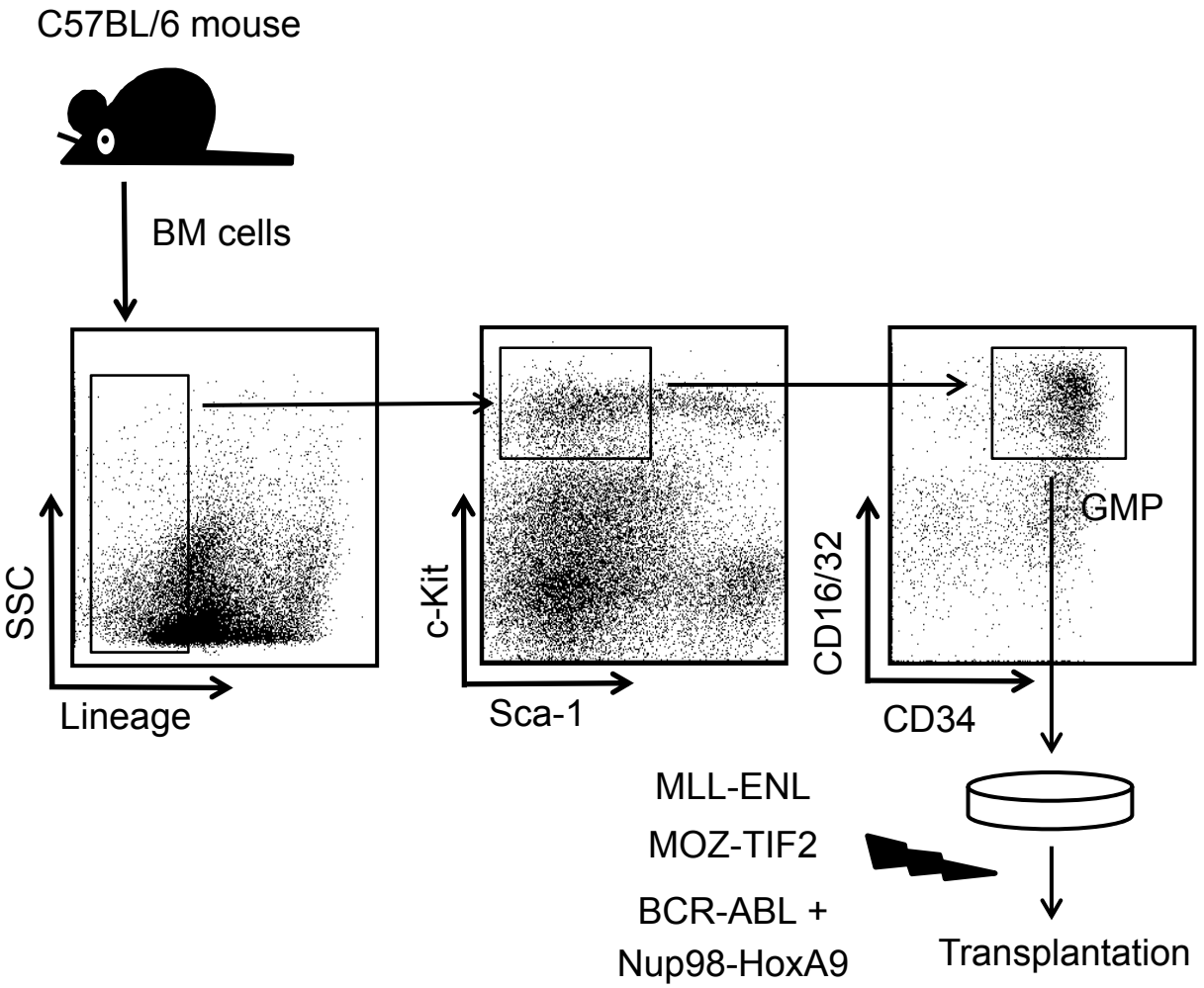

Supplemental Figure 1. Generation of three myeloid leukemia mouse models. Bone marrow granulocyte-monocyte progenitors (GMP) isolated from C57BL/6 mice were transduced with MLL-ENL, MOZ-TIF2, or BCR-ABL + Nup98-HoxA9 and transplanted into irradiated recipient mice.

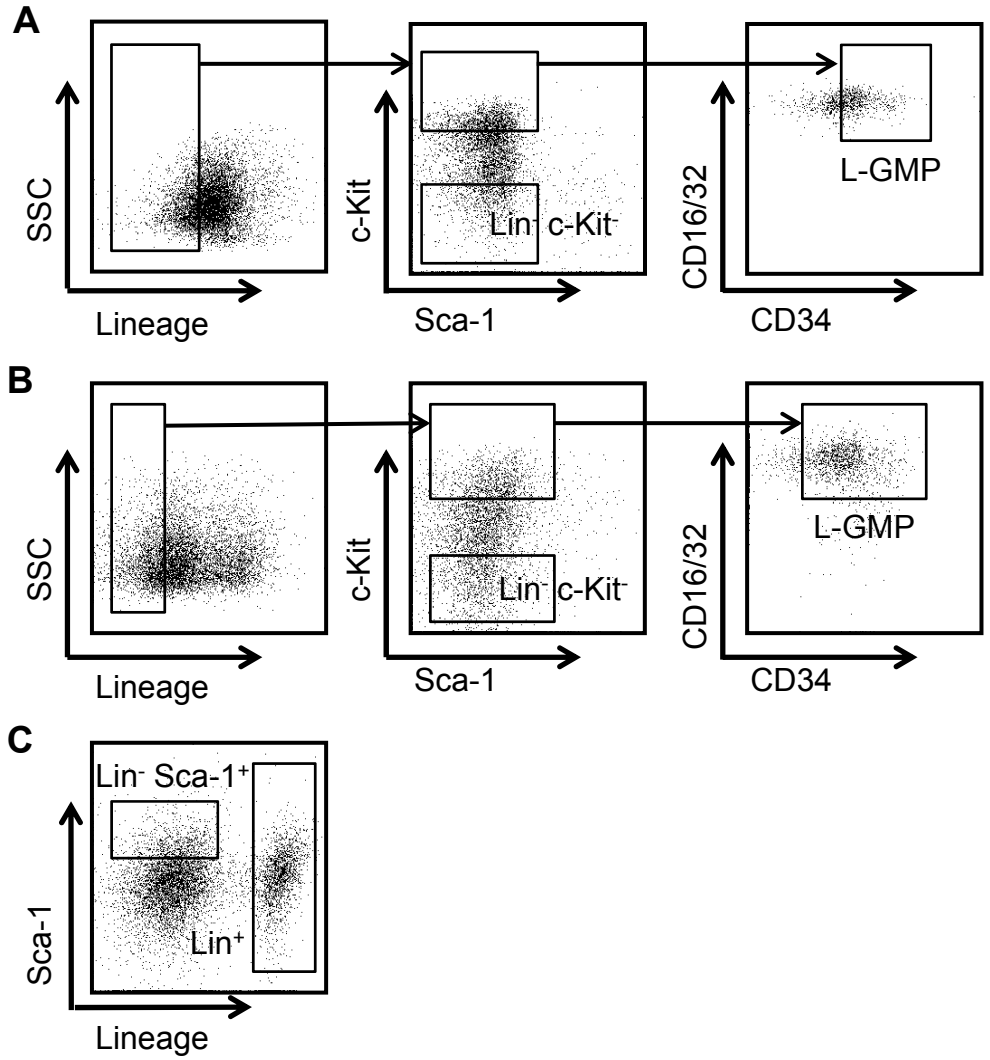

Supplemental Figure 2. Isolation of LIC and non-LIC from each leukemia model. (A, B) L-GMP and Lin$^-$ c-Kit$^-$ fractions were isolated from MLL-ENL (A) and MOZ-TIF2-induced leukemia mice (B). (C) Lin$^-$ Sca-1$^+$ and Lin$^+$ fractions were isolated from BCR-ABL/Nup98-HoxA9-induced leukemia mice.

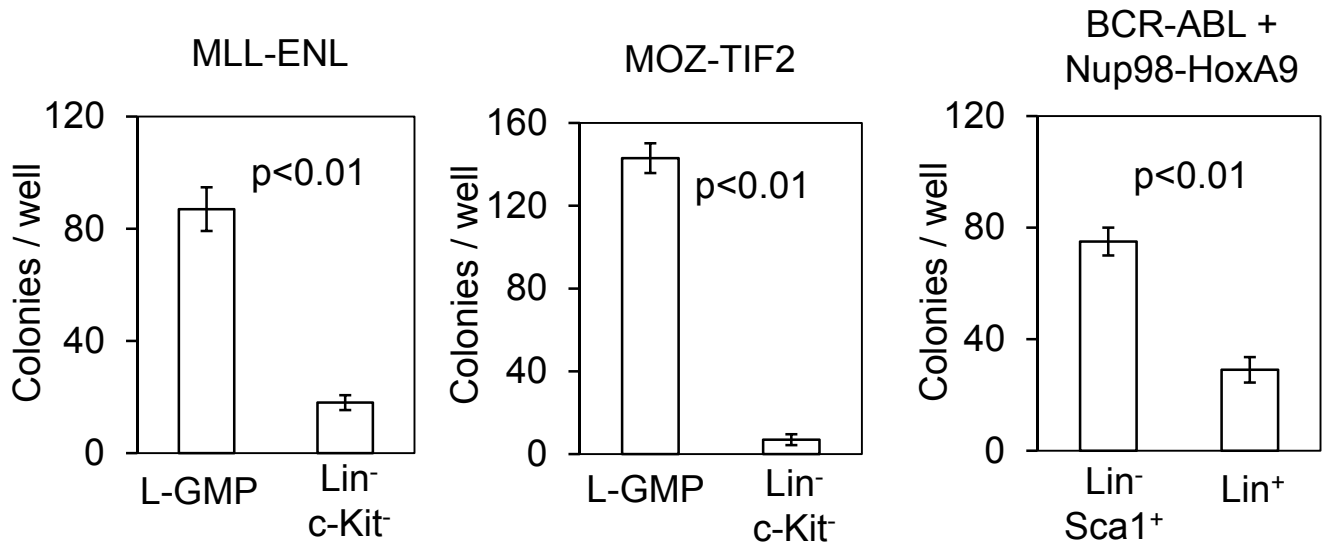

Supplemental Figure 3. Colony-forming cell assay in the two fractions from each leukemia model (n=3 each). Cells were seeded at 200 cells per well in MLL-ENL or MOZ-TIF2-induced leukemia cells, and at 1000 cells per well in BCR-ABL/Nup98-HoxA9-induced leukemia mice. Error bars indicate SD.

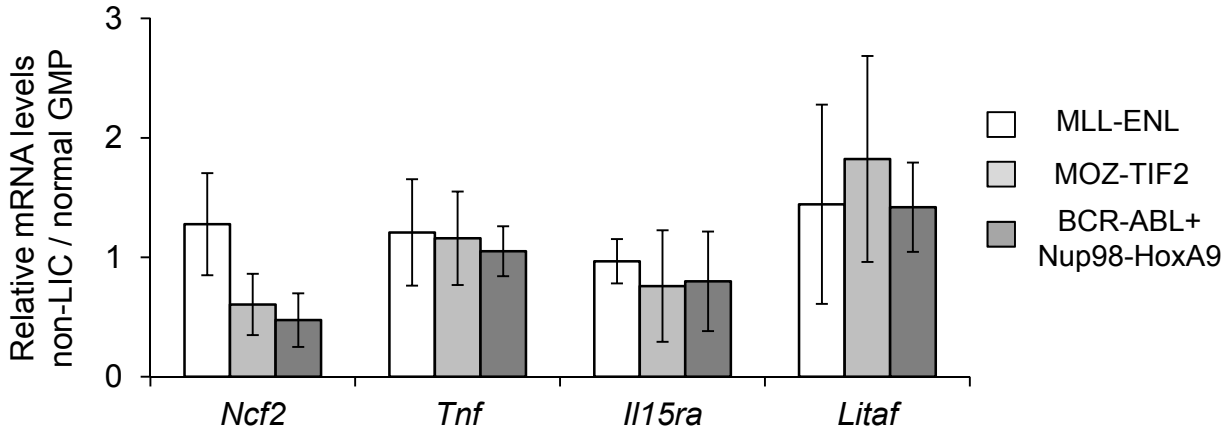

Supplemental Figure 4. Quantitative real-time PCR analysis of a subset of NF-κB target genes in non-LIC of MLL-ENL, MOZ-TIF2, and BCR-ABL/Nup98-HoxA9-induced leukemia models relative to normal GMP (n=4 each). Error bars indicate SD.

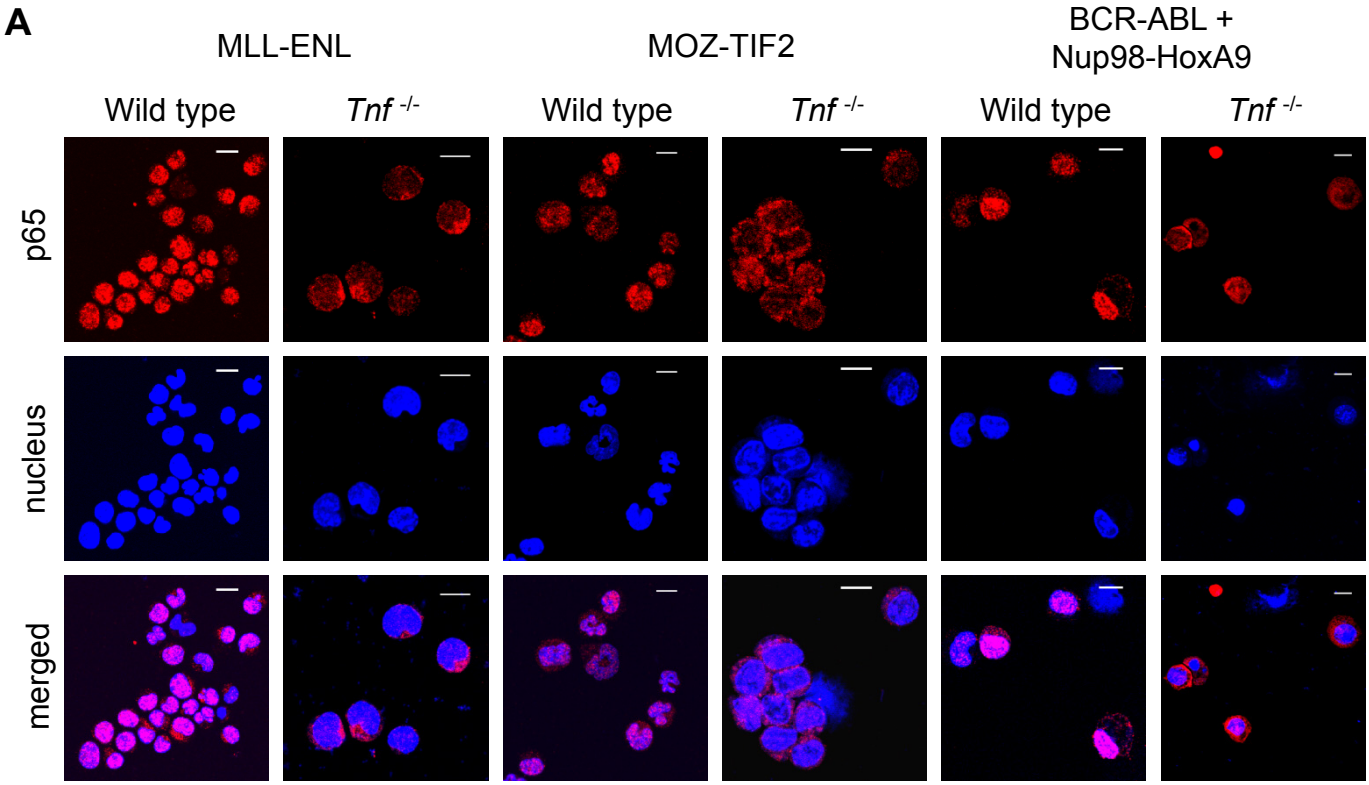

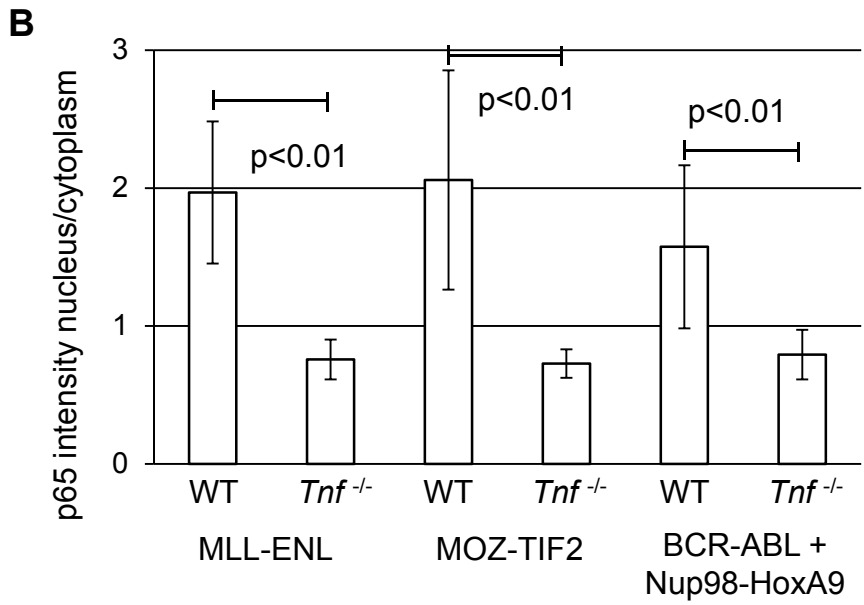

Supplemental Figure 5. NF-κB pathway activity is attenuated in *Tnf*-deficient LIC. (A) Immunofluorescence assessment for p65 nuclear translocation in LIC of three leukemia models established from wild-type or *Tnf*$^{-/-}$ mice. Scale bar, 10 μm. (B) Quantification of p65 nuclear translocation assessed by the mean intensity ratio between nucleus and cytoplasm. More than 50 cells were scored in each specimen and the average intensity ratio with SD is shown.

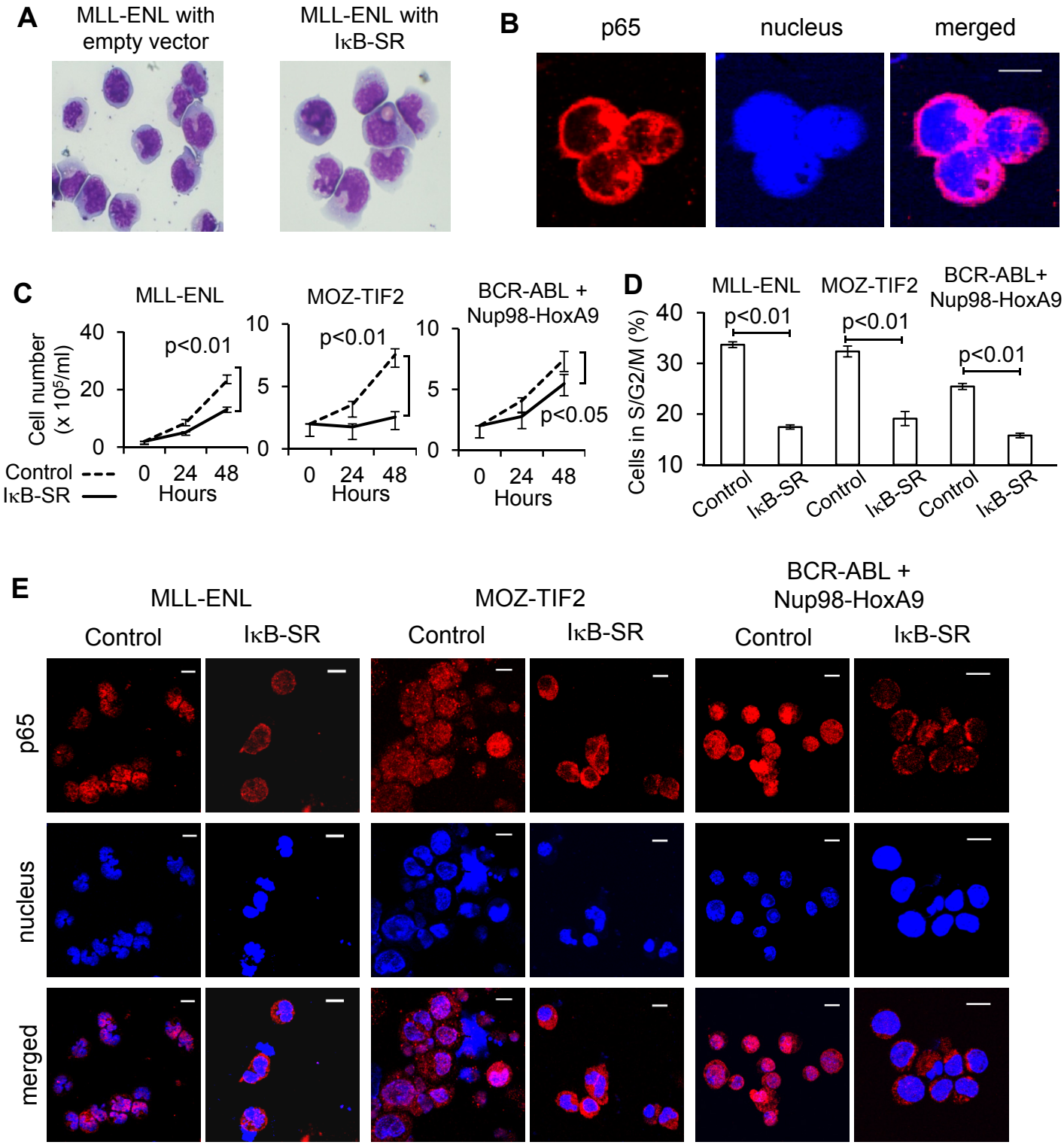

Supplemental Figure 6. Influence of NF-κB inhibition on leukemia cells. (A) Leukemic bone marrow mononuclear cells of MLL-ENL leukemia with IκB-SR stained with Wright-Giemsa. (B) Immunofluorescence staining of p65 in MLL-ENL L-GMP with IκB-SR. Scale bar, 10 μm. (C, D) Cell cycle analysis (C) and proliferation status (D) of leukemia cells with or without IκB-SR (n=3 in each experiment). (E) Immunofluorescence staining of p65 in LIC with or without IκB-SR recovered from secondary recipient mice. Scale bar, 10 μm.

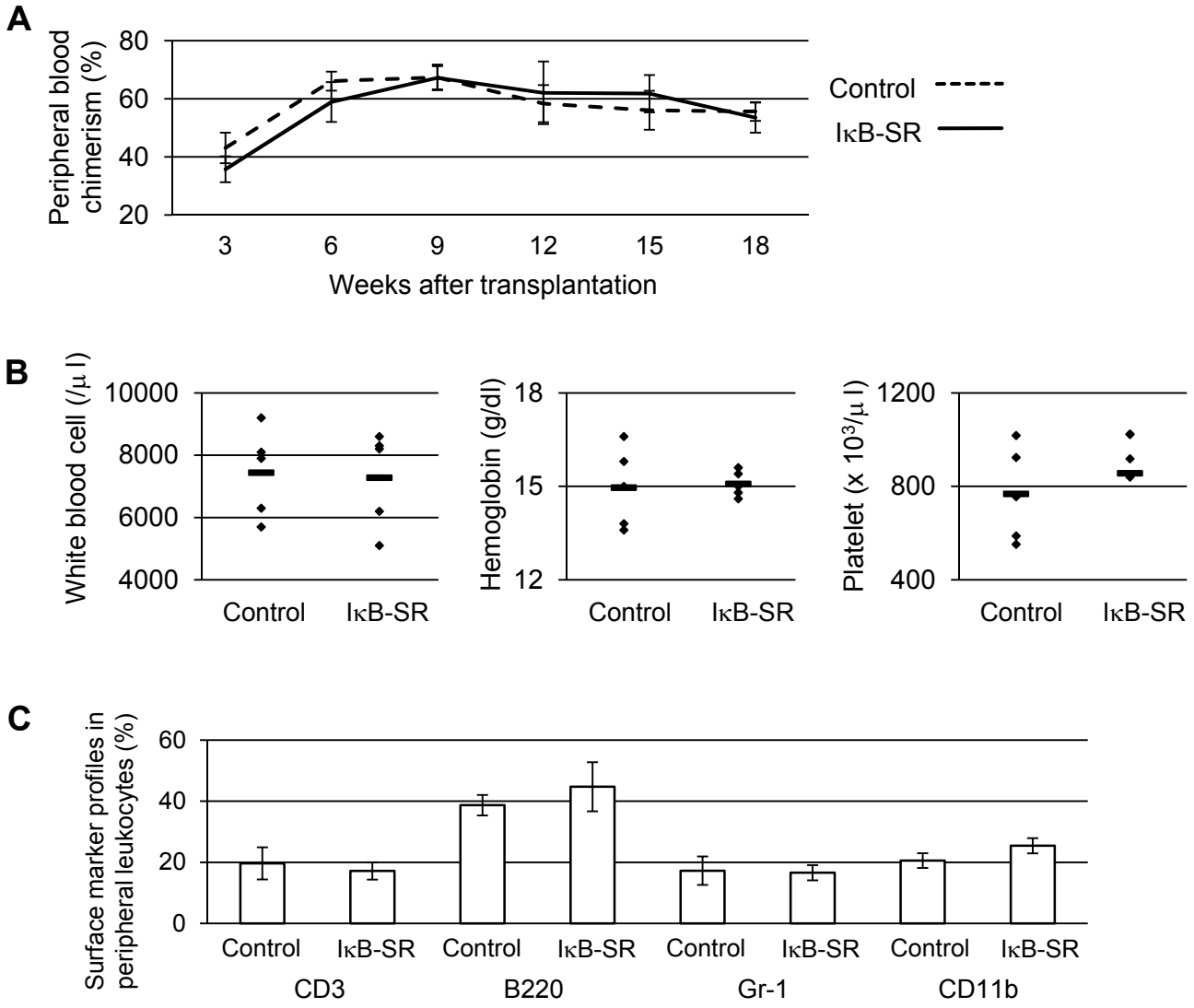

Supplemental Figure 7. Influence of NF-κB inhibition on normal hematopoietic cells. (A-C) Normal c-Kit$^+$ bone marrow cells were transduced with IκB-SR-IRES-Kusabira Orange or empty vector and transplanted into lethally irradiated mice. Peripheral blood Kusabira Orange positivty was monitored after transplantation (A). Complete blood cell counts (B) and surface marker profiles in peripheral leukocytes (C) were examined in individual mice 18 weeks after transplantation.

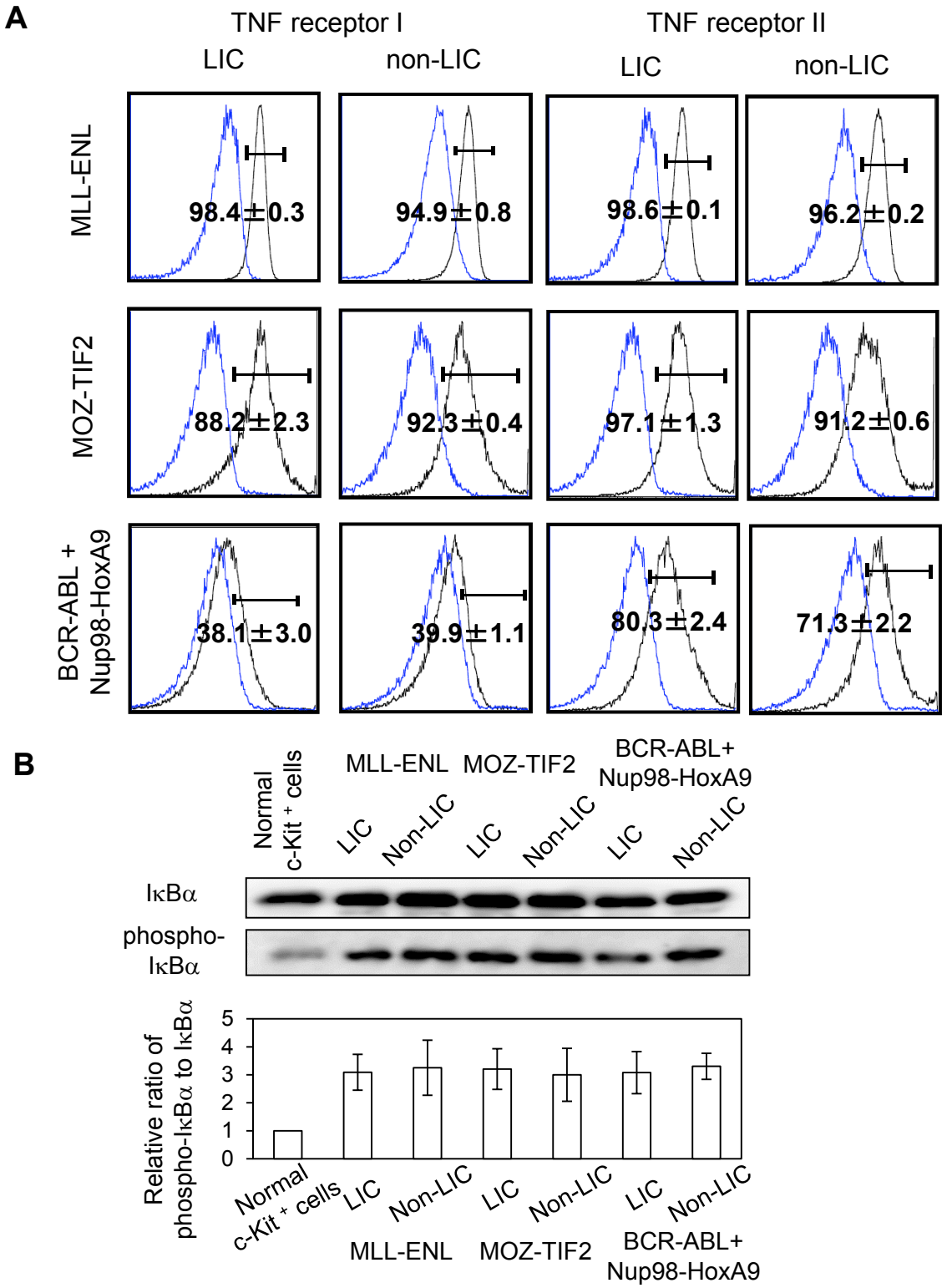

Supplemental Figure 8. Comparison of TNF receptors expression and IKK activity between LIC and non-LIC. (A) Expression of TNF receptors in LIC and non-LIC of each leukemia model. Representative FACS plots and average percent positive ± SD are shown (n=3 each). Blue lines represent the isotype control. (B) Immunoblotting of IκBα and phosphorylated form of IκBα in normal c-Kit$^+$ cells, LIC and non-LIC in different types of leukemia cells two hours after treatment with 20 μM MG132. Protein levels were quantified with ImageJ software and the relative ratio of phosphorylated IκBα to total IκBα compared with those of normal cells were calculated (n=3 each). Error bars indicate SD.

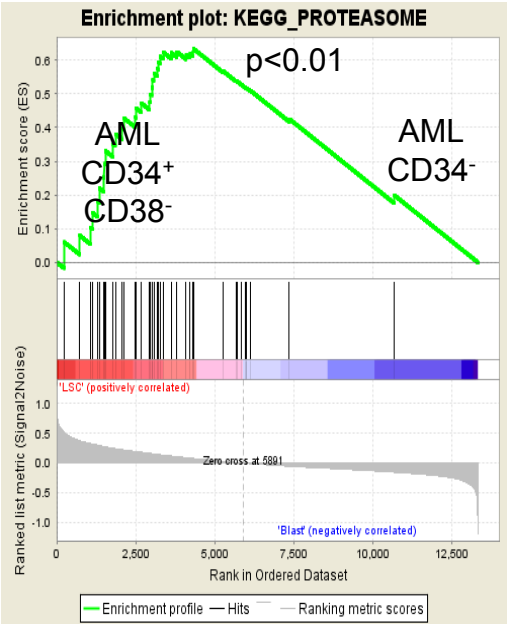

Supplemental Figure 9. Gene set enrichment analysis for expression profiles of proteasome subunits: comparison of $CD34^+$ $CD38^-$ cells with $CD34^-$ leukemia cells in human AML samples.

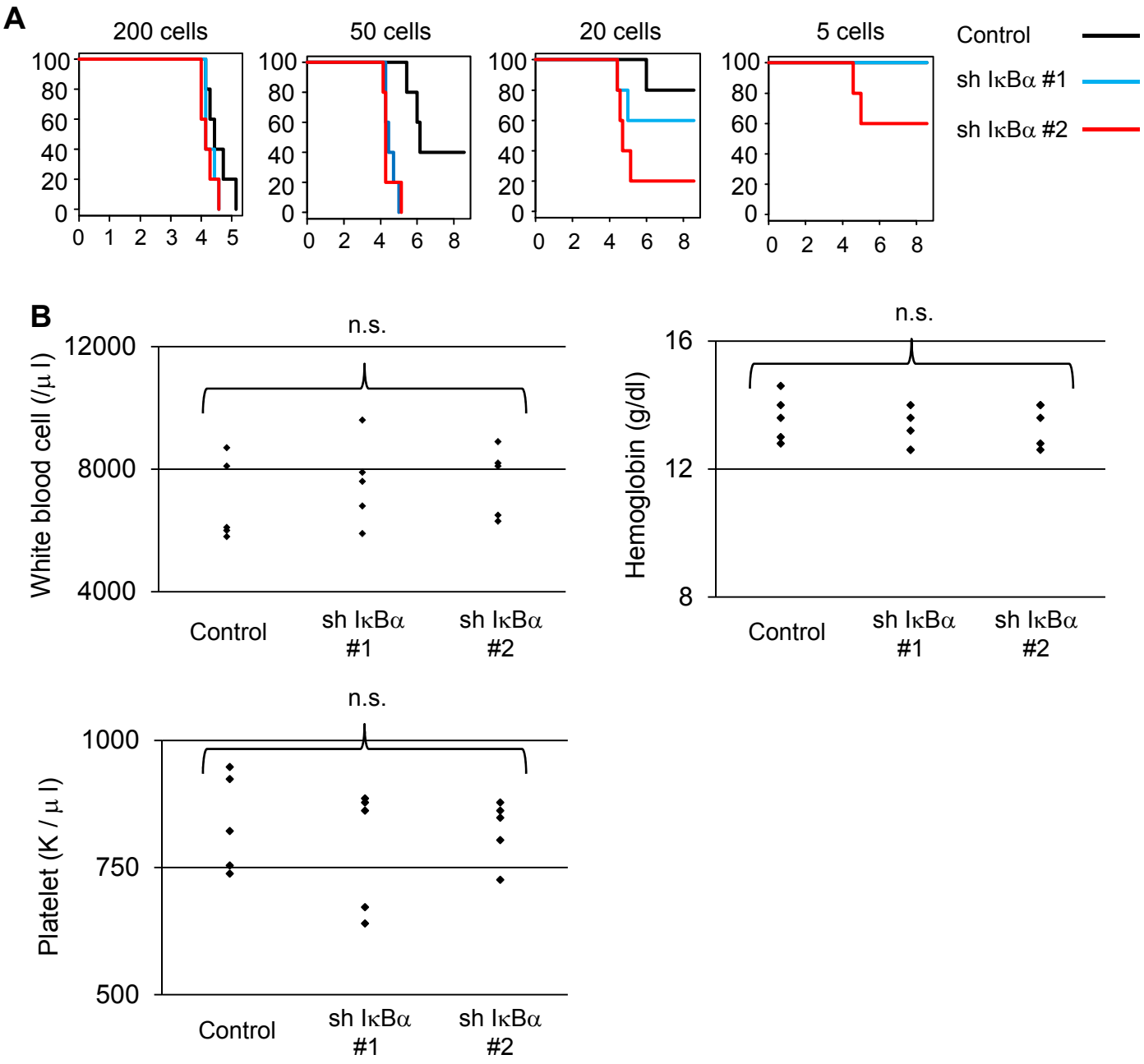

Supplemental Figure 10. Influence of IκBα knockdown on leukemia progression and normal hematopoiesis. (A) Limiting dilution transplant assay of bone marrow mononuclear cells derived from MLL-ENL-IκBα^{KD} leukemia mice compared with control mice. (B) Peripheral blood cell counts in mice transplanted with normal c-Kit^{+} cells with shRNA against IκBα or control shRNA. Data at 18 weeks after transplantation are shown (n=5 each).

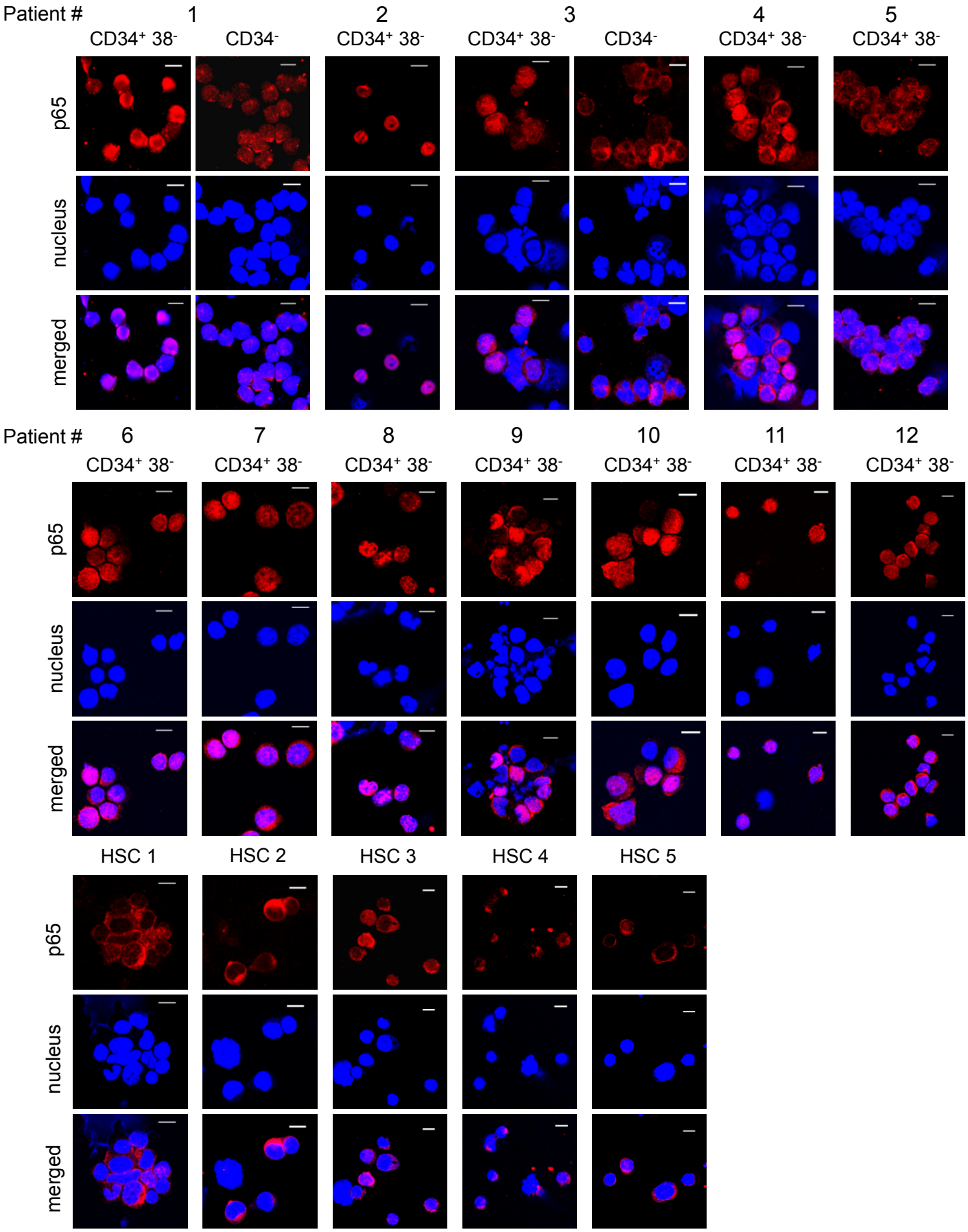

Supplemental Figure 11. Immunofluorescence assessment for p65 nuclear translocation of $CD34^+$ $CD38^-$ cells or $CD34^-$ cells isolated from 12 patients with AML and 5 normal controls. Scale bar, 10 μm.

Supplemental Table 1

Limiting dilution transplantation assay data.

Leukemia model	Cell population	Transplanted cells	Incidence of leukemia (%)
MLL-ENL	L-GMP	1000	4/4 (100)
		100	4/4 (100)
		20	4/4 (100)
		5	2/5 (40)
	Lin^- $c\text{-}Kit^-$	10000	4/4 (100)
		1000	3/4 (75)
		200	2/4 (50)
		20	0/4 (0)
MOZ-TIF2	L-GMP	10000	4/4 (100)
		1000	4/4 (100)
		100	2/6 (33)
		20	0/4 (0)
	Lin^- $c\text{-}Kit^-$	500000	4/4 (100)
		100000	2/6 (33)
		10000	0/4 (0)
BCR-ABL + Nup98-HoxA9	Lin^- $Sca1^+$	10000	4/4 (100)
		1000	4/4 (100)
		200	4/4 (100)
		20	3/4 (75)
	Lin^+	10000	4/4 (100)
		1000	1/4 (25)
		200	0/4 (0)
		20	0/4 (0)

Supplemental Table 2

Previously investigated NF-κB-regulated genes.

Gene symbol	Gene full name
EMR1	egf-like module containing, mucin-like, hormone receptor-like 1
CD86	CD86 molecule
CD44	CD44 molecule (Indian blood group)
IL15RA	interleukin 15 receptor, alpha
CD40	CD40 molecule, TNF receptor superfamily member 5
CCR7	chemokine (C-C motif) receptor 7
ICAM1	intercellular adhesion molecule 1 (CD54), human rhinovirus receptor
CD83	CD83 molecule
IER3	immediate early response 3
BCL2L1	BCL2-like 1
BCL2A1	BCL2-related protein A1
FAS	Fas (TNF receptor superfamily, member 6)
BIRC3	baculoviral IAP repeat-containing 3
TRAF1	TNF receptor-associated factor 1
RRAS2	related RAS viral (r-ras) oncogene homolog 2
TNIP1	TNFAIP3 interacting protein 1
PRKCD	protein kinase C, delta
SMAD7	SMAD, mothers against DPP homolog 7 (Drosophila)
LSP1	lymphocyte-specific protein 1
IRF1	interferon regulatory factor 1
SPIB	Spi-B transcription factor (Spi-1/PU.1 related)
STAT5A	signal transducer and activator of transcription 5A
NFKB2	nuclear factor of kappa light polypeptide gene enhancer in B-cells 2 (p49/p100)
NCF2	neutrophil cytosolic factor 2 (65kDa, chronic granulomatous disease, autosomal 2)
RFTN1	raftlin lipid raft linker 1
SLC2A5	solute carrier family 2 (facilitated glucose/fructose transporter), member 5
TFPI2	tissue factor pathway inhibitor 2
AMPH	amphiphysin (Stiff-Man syndrome with breast cancer 128kDa autoantigen)
NOP14	nucleolar protein homolog (yeast)
WTAP	Wilms tumor 1 associated protein
PASK	PAS domain containing serine/threonine kinase
TPMT	thiopurine S-methyltransferase
STX4	syntaxin 4
HLAF	major histocompatibility complex, class I, F
LITAF	lipopolysaccharide-induced TNF factor
LTA	lymphotoxin alpha (TNF superfamily, member 1)

CX3CL1	chemokine (C-X3-C motif) ligand 1
IL13	interleukin 13
CCL3	chemokine (C-C motif) ligand 3
CSF2	colony stimulating factor 2 (granulocyte-macrophage)
CCL22	chemokine (C-C motif) ligand 22
IL6	interleukin 6 (interferon, beta 2)
TNF	tumor necrosis factor (TNF superfamily, member 2)
CCL1	chemokine (C-C motif) ligand 1